Abstract of Paper No: 125

Response of FRP-glulam slab systems under five-point bending load

Marco Jorge[1], Jorge Branco[1], José Sena-Cruz[1], Joaquim Barros[1] and Gláucia Dalfré[1]

[1] *ISISE, University of Minho, Department of Civil Engineering, Guimarães, Portugal*

In the last decades the use of fiber reinforced polymers (FRPs) in the context of repairing and strengthening structures has been significantly increased. Properties such as light weight, high stiffness/weight ratio, corrosion immunity and wide variety of available sizes and shapes are some of the reasons that justify the growing use of this type of materials. FRP's are being used for the strengthening of concrete, masonry, steel and wood structures.

To characterize flexural response of FRP-glulam structural systems, an experimental program was carried out. For that purpose, strips of slabs with a two-span continuous configuration were subjected to five-point bending loads, and the effectiveness of two strengthening techniques was analyzed: the externally bonded reinforcement (EBR) and the near-surface mounted (NSM) reinforcement. Glass fiber reinforced polymers (GFRP) were used in both strengthening techniques and two distinct levels of strengthening were studied: increasing the load carrying capacity of 20% and 40%, when compared with the unstrengthened slabs.

The test configuration includes the use of glulam slabs with 90 mm thick, 400 mm wide and 5800 mm long. The distance between loading points is 1400 mm. The monitoring system included the measurement of the slab deflection in critical sections using displacement transducers (LVDT's), the strains in pre-selected points of the glulam slab and in FRP's sections through strain gauges, and the applied loads using load cells. The tests were performed using servo controlled equipment, under displacement control.

The present work describes the tests carried-out, and presents and analyzes the most significant obtained results.

Corresponding author's email: jsena@civil.uminho.pt

Response of FRP-glulam slab systems under five point bending load

Marco Jorge[1], Jorge Branco[1], José Sena-Cruz[1], Joaquim Barros[1] and Gláucia Dalfré[1]

[1] ISISE, University of Minho, Department of Civil Engineering, Guimarães, Portugal

ABSTRACT: Full-scale slab strips were tested in order to analyze the flexural response of FRP-glulam slab systems under monotonic loading. The type of strengthening technique (externally bonded reinforcement – EBR and near-surface mounted – NSM) and the increase target in terms of ultimate load capacity (20% and 40%) were the main studied parameters. GFRP sheets were utilized in the EBR technique, while GFRP rods were applied in NSM technique. In this work the tests are described in detail, and the obtained results are presented and discussed.

1 INTRODUCTION

Glued laminated (glulam) timbers appear for the first time at the beginning of the XX century, by Otto Hetzer. Since then, glued laminated technology faced great improvements. Nowadays, the manufacturing process of glulam is strict and industrialized, which makes the geometry very precise, controlled moisture content and mechanical properties with less dispersion. This leads to a higher mechanical resistance and elasticity modulus when comparing to solid wood. Glulam materials have widely been used in transportation infrastructures (e.g. bridges), and in roofs of pavilions.

In the last two decades, fiber reinforced polymer (FRP) materials have been tested and used to repair or strengthen existing structures. High stiffness and tensile strength, low weight, easy installation procedures, high durability (no corrosion), electromagnetic permeability and practically unlimited availability in terms of geometry and size are the main advantages of these composites, ACI (2008).

In the literature it can be found some applications and studies of FRP-glulam systems (Davalos et al. (1992), Dagher et al. (1996), Tingley et al. (1997), Dagher et al. (1998), Dagher and Lindyberg (1999), Brody et al. (2000), Lopez-Anido and Xu (2002)). In some cases it was found that the FRP-glulam beams with sufficient reinforcement in the tension regions not only exhibit significant strength increment, but also they develop wood ductile compression failure, rather than the typical brittle tension failure of wood (Dagher et al. (1996), Dagher and Lindyberg (1999), Lopez-Anido and Xu (2002)).

In this context, the effectiveness of flexural strengthening configurations for glulam continuous slab strips of two equal span lengths was explored in terms of load carrying capacity and moment redistribution. For that purpose, six full-scale glulam slab strips were tested. The type of strengthening technique (EBR and NSM) and the increase level of load carrying capacity (20% and 40%) to be attained are the main parameters considered in this experimental program. GFRP sheets were used in the EBR technique, while GFRP rods were applied in the NSM

technique. In the following sections the tests are described in detail, and the obtained results are presented and discussed.

2 EXPERIMENTAL PROGRAM

2.1 Test specimens

The six full-scale two span glulam slab strips are organized in three different series. The first series is composed by two unstrengthened slabs (reference slabs, REF_1 and REF_2). The second series is composed by two glulam slab strips strengthened according to the NSM GFRP using a percentage of GFRP rods in an attempt to increase the maximum load in 20% (NSM_20 and 40% (NSM_40), when compared to the one registered in the average of REF1 and REF2. Finally, in the third series two glulam slab strips were strengthened according to the EBR technique applying GFRP sheets, and the purpose was also to increase the maximum load in 20% (EBR_20) and 40% (EBR_40), respectively.

Fig. 1 depicts the test setup in terms of load configuration, support conditions and measuring devices. Fig. 1(b) indicates the six linear voltage differential transducers (LVDT's) used to measure the deflections of the slab strips. The LVDT's 60541 and 18897, placed at the slab loaded sections, were used to control the test at a displacement rate of 20 μm/s. The load (F_{522}) applied at the left span (see Fig. 1(a)) was measured using a load cell of ±200 kN and accuracy of ±0.03%. In the right span, the load (F_{123}) was measured using a load cell of ±250 kN and accuracy of ±0.05%. To monitor the reaction forces, load cells were installed at two supports. One load cell (AEP_200) was positioned at the central support (nonadjustable support), placed between the reaction steel frame (HEB 300 profile) and the slab's support device (see Fig. 1(b)). The other load cell (MIC_200) was positioned in-between the reaction steel frame and the apparatus of the adjustable right support of the slab. These cells have a load capacity of 200 kN and accuracy of ±0.05%. Fig. 2 presents the transverse geometry and the strengthening arrangements of the tested slabs, whereas Fig. 3 presents the longitudinal configuration of the strengthened slabs and the corresponding strain gauges locations.

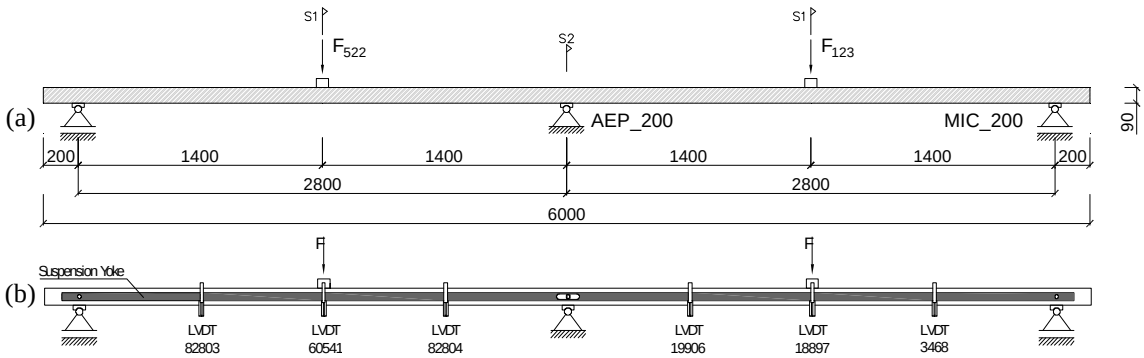

Figure 1. (a) Test configuration; (b) displacement transducers location. All dimensions in [mm].

2.2 Characterization of the materials

In the present experimental program glued laminated timber of strength class GL24h (NP EN 1194:1999) was used for all the series. The material characterization of the GL24h included compression and tension tests parallel to the grain according to EN 408 (CEN 2003). From the compression tests an average compressive strength of 27.99 MPa with a coefficient of variation (CoV) of 17.6% and an average modulus of elasticity of 6.62 GPa (CoV=27.8%) were obtained. From the tension tests, an average tensile strength, modulus of elasticity and strain at the peak stress of 55.93 MPa (CoV=16.7%), 9.17 GPa (CoV=11.9%) and 6.35‰ (CoV=12.4%) were obtained, respectively.

The GFRP rod used in the present work, with a trademark Maperod G, is provided in rolls with 6 meters each and it is produced by MAPEI®. These rods have a diameter of 10 mm and the external surface is sand blasted. Tension tests were carried out to assess the tensile mechanical properties of GFRP rod according to ISO TC 71/SC 6 N - Part 1 (2003). Tests were performed at a displacement rate of 2 mm/min. To measure the modulus of elasticity, a clip gauge was mounted at middle region of each specimen. From the experimental tests an average tensile strength of 778.14 MPa (CoV=3.5%), an average modulus of elasticity of 38.42 GPa (CoV=1.3%) and an average ultimate strain of 20.25‰ (CoV=2.3%) were obtained.

The unidirectional GFRP sheets used in this study was provided in rolls with 100 meters long and 0.6 meters wide and it was produced by MAPEI®. The GFRP sheet has the trademark MapeWrap G UNI AX 900/60 and its tensile behavior was assessed by uniaxial tensile tests carried out according to TC 71/SC 6 N - Part 2 (2003) recommendations. An average tensile strength of 2209.60 MPa (CoV=13.86%), an average elasticity modulus of 101.20 GPa (CoV=4.31%) and an average ultimate strain of 21.79‰ (CoV=11.32%) were obtained.

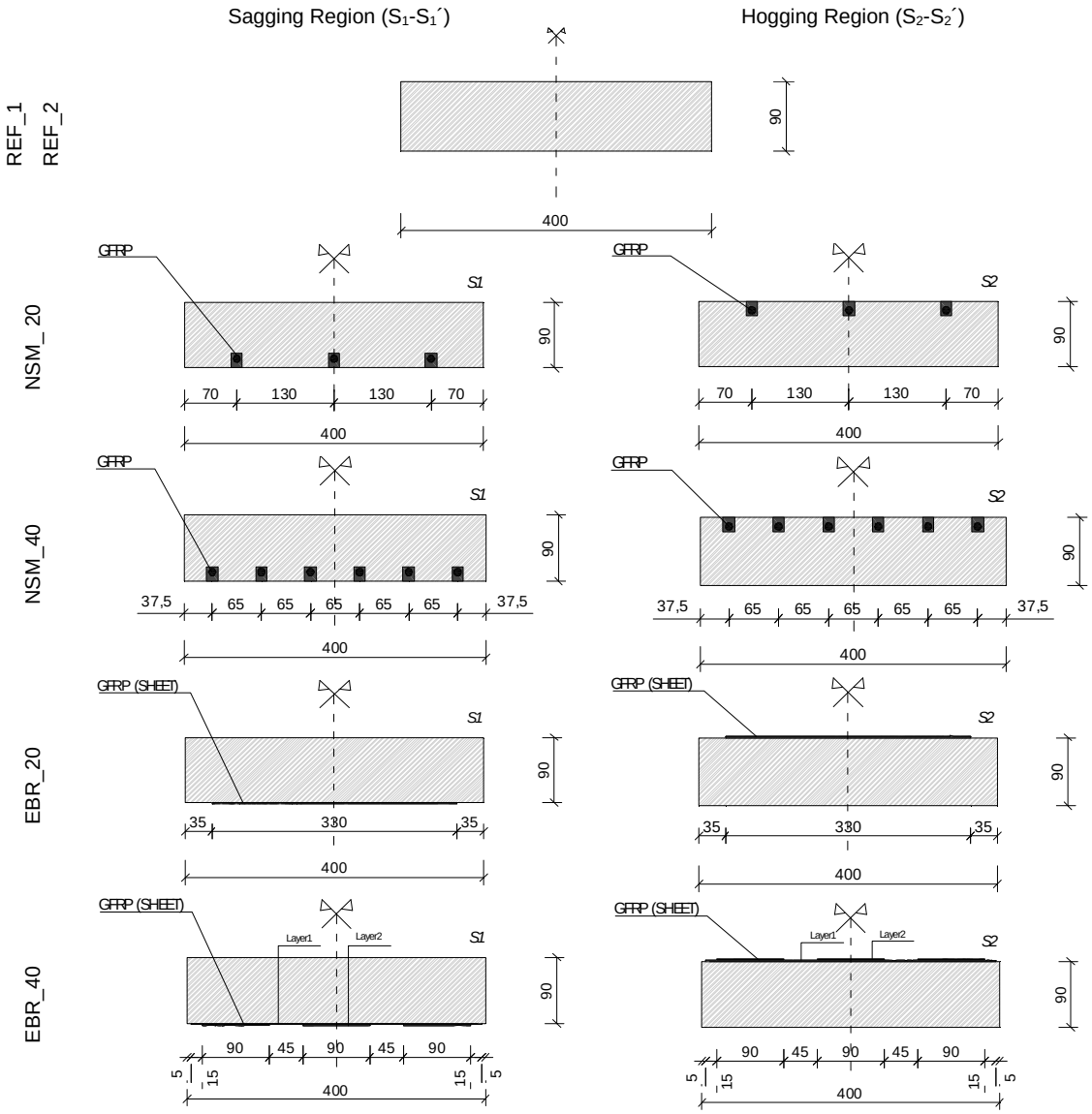

Figure 2. Specimens cross-sectional dimensions of sagging (S1-S1') and hogging regions (S2-S2'). All dimensions in [mm].

Two distinct adhesives were used in the experimental program: MapeWrap 31 and MapeWood Paste 140, being both supplied by MAPEI®. The former adhesive is a medium viscosity epoxy resin for the impregnation of FRP sheets, whereas the last is a thixotropic epoxy adhesive currently used in the restoration of timber structural elements. The MapeWrap 31 was used with the EBR strengthening technique, while the MapeWood Paste 140 was adopted to bond the NSM rods. To assess the tensile properties of each hardened adhesives, six tensile tests for each experimental series were carried out according to ISO 527-2 (1993). After casted, the adhesive specimens were kept in the laboratory environment, as the slab specimens, and were tested after the same curing period of time of the strengthening intervention process of the corresponding slabs when tested. A universal test machine was used with a displacement rate of 1 mm/min. A clip gauge mounted on the middle zone of the specimen recorded the strains, whereas a high accurate cell load has registered the applied force. The obtained results are presented in Table 1.

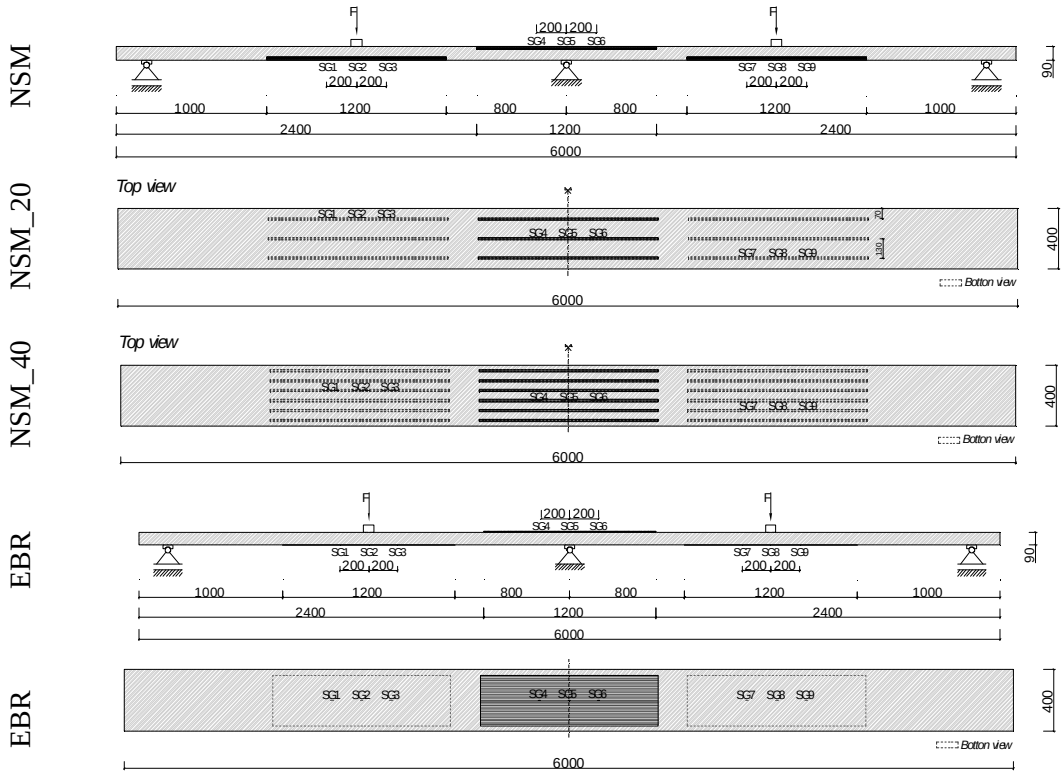

Figure 3. Longitudinal configuration of the strengthened slabs. All dimensions in [mm].

Table 1. Main results obtained on the mechanical characterization of the adhesive (average values)

Adhesive	F_{fmax} (kN)	σ_{fmax} (MPa)	E_f (GPa)	ε_{fmax} (‰)
MapeWood Paste 140	0.65 (5.5%)	15.41 (4.3%)	6.49 (2.6%)	2.82 (9.4%)
MapeWrap 31 (Specimen EBR_20)	1.75 (3.8%)	44.33 (4.0%)	2.77 (5.2%)	18.95 (10.5%)
MapeWrap 31 (Specimen EBR_40)	1.62 (8.8%)	40.47 (8.6%)	2.58 (3.2%)	17.33 (11.9%)

Notes: $F_{adh,max}$= maximum force; $\sigma_{adh,max}$= uniaxial tensile strength; E_{adh}= longitudinal elasticity modulus; $\varepsilon_{adh,max}$= strain at σ_{fmax}; E_{adh} is the slope of the curve σ–ε between 0.0025 and 0.0075 of ε. The values between parentheses are the corresponding coefficients of variation.

3 PREPARATION OF THE SPECIMENS

3.1 NSM strengthening technique

The main steps of the specimen's preparation are briefly described. The GFRP bars were installed into grooves of 15 mm wide and 20 mm deep, opened in the glulam, on the top face of the hogging region and on the bottom face of the sagging regions, by using a Hilti diamond saw cutter machine. To eliminate splinters and dust resultant from the cutting process, sandpaper was applied inside the grooves and they were then cleaned using compressed air. The GFRP rods were also cleaned with acetone to remove any possible dirt, and strain gauges were glued in the predefined locations. The FRP rods were glued to the glulam using the MapeWood Paste 140 epoxy adhesive. The grooves were filled with the epoxy adhesive using a spatula, followed by the application of a thin layer of adhesive on the FRP surface. The rods were then gradually introduced into the grooves until its final position at about 75 mm from the external surface. Further information can be found in Jorge (2010).

3.2 EBR strengthening technique

To eliminate splinters and dust, a sanding process with sandpaper was applied in the zones where the FRP's systems were planned to be installed, followed by the application of compressed air. The GFRP sheets were cut with the desired dimensions and cleaned with acetone. The GFRP sheets were glued to the glulam using the MapeWrap 31 epoxy adhesive. The sheets were impregnate with the epoxy adhesive using a broche, and a hard rubber roller was used to press the sheet to remove possible voids. After curing, strain gauges were installed on the GFRP sheet surface. Further information can be found in Jorge (2010).

4 RESULTS

The obtained results were analyzed in terms of maximum load, F_{max}, deflection at the peak load, δ_{max}, failure modes and moment redistribution index, η, which is obtained from:

$$\eta = 1 - \delta = 1 - \frac{M_{red}}{M_{elast}} = 1 - \frac{2.8 \cdot F_{MIC} - 1.4 \cdot F_{123}}{(5/6 \cdot 2.8 - 1.4) \cdot F_{123}} \quad (1)$$

where M_{red} is the bending moment in the intermediate support after moment redistribution, and M_{elast} is the bending moment in this section, calculated according to the theory of elasticity. Fig. 4 presents the F-δ curves, whereas Table 2 summarizes the obtained results.

4.1 Reference slabs

The load *versus* deflection curves, F-δ, obtained in both tests are presented in Fig. 4a-b. Despite the symmetry of the test setup, the response of the glulam slabs strips is not symmetric. The maximum values obtained for the average applied load are similar (46.28 kN and 47.23 kN for REF_1 and REF_2, respectively). The behaviour is linear elastic until failure (brittle behaviour), which occurred in the hogging region. After the formation of the first cracks in the hogging region, quite smaller bending moment redistribution was obtained for the reference slabs (average value of 2.5%).

4.2 NSM series

When compared with the unstrengthened slabs, in NSM_20 and NSM_40 the response obtained for both spans was more similar. However, the most important effect of this strengthening technique is the non-linear F-δ response, as visible in Fig. 4c-d. In fact, the full linear elastic response obtained for the unstrengthened slabs strips is replaced by an elasto-plastic behavior,

with a significant plastic branch (ductility). The NSM_20 slab strip has achieved a maximum average applied load (F_{max}) of 47.32 kN for a deflection of 53.90 mm, representing only an increment of 1.2% in the applied load and 15.0% in the corresponding deflection. Concerning to the NSM_40 slab strip, a maximum average applied force of 53.99 kN was attained with a corresponding deflection of 76.94 mm. At the peak load, a moment redistribution of about 10% and 25% was obtained for the NSM_20 and NSM_40, respectively.

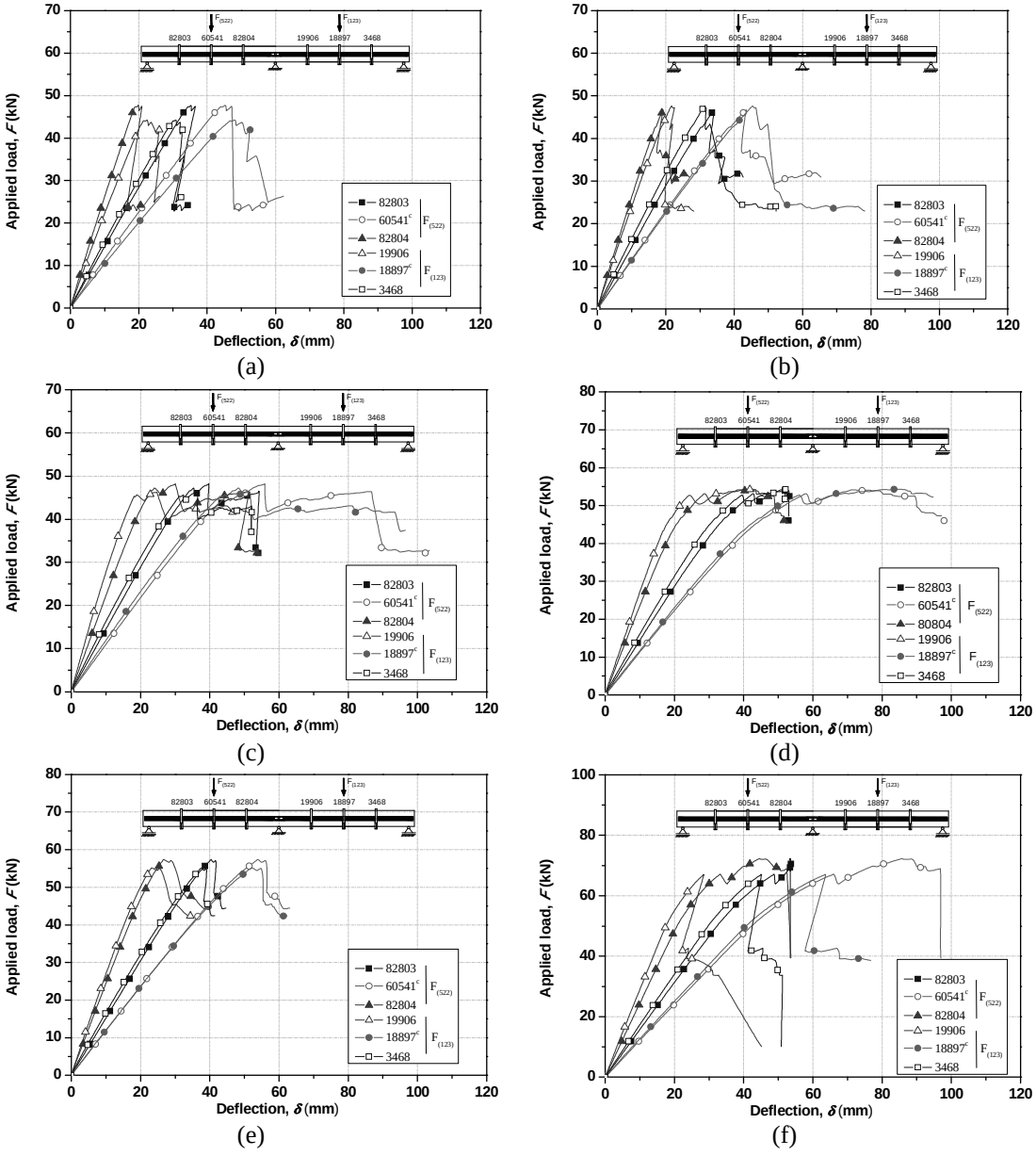

Figure 4. Curves F-δ of the (a) REF_1, (b) REF_2, (c) NSM_20, (d) NSM_40, (e) EBR_20 and (f) EBR_40 specimens.

4.3 EBR series

Fig. 4e-f shows the F-δ curves, where a quite symmetric response of the slabs can be observed. The EBR_20 presented an ultimate average load of 56.54 kN for a deflection of 53.34 mm, representing an increment of 20.9% in the applied load and 13.9% in the corresponding deflection, while the moment redistribution at the peak load was of about 10%. Concerning to the EBR_40 slab strip, a maximum average load of 67.33 kN was obtained, for a deflection of

65.22 mm, representing an increment of 44.0% in the applied load and 39.2% in the corresponding deflection. A moment redistribution of about 9% was obtained at the peak load for both strengthened slab strips. According to the Fig. 4e-f, the behavior is linear elastic until the maximum load, after which a sudden drop in the load carrying capacity is observed, revealing a behavior without ductility (fragile failure). This behavior is confirmed by the linear variation registered during these tests between the applied load and the strains in the SGs installed in the both GFRP sheets and glulam, Jorge (2010). In consequence, no significant local embedment of wood was observed in the compression side.

Table 2. Main results obtained in the tests.

Slab	F_{max} (kN)	δ_{max} (mm)	η (%)
REF_1+REF_2	46.75	46.85	5%
NSM_20	47.32 (+1.2%)	53.90 (+15.0%)	10%
NSM_40	53.99 (+15.4%)	76.94 (+64.2%)	25%
EBR_20	56.54 (+20.9%)	53.34 (+13.9%)	9%
EBR_40	67.33 (+44.0%)	65.22 (+39.2%)	9%

4.4 Failure modes

Representative failure modes for all the tested series (REF, NSM and EBR) are depicted in Fig. 6. The unstrengthened specimens did not show local embedment in the compression regions. The failure occurred in the tension side. In consequence of the brittle nature of the timber behavior in tension, the failure is sudden and violent.

The slabs strips strengthened with the NSM technique have showed an extensive cracking located at the existing wood between the FRP rods. Tension cracks have formed in the hogging and saggings regions, despite being more evident in the hogging, and always local embedment in the compression side was observed in the hogging region.

For the EBR series, the failure always occurred by debonding of FRP. Local embedment in the compression region was only observed in the EBR_40 specimen.

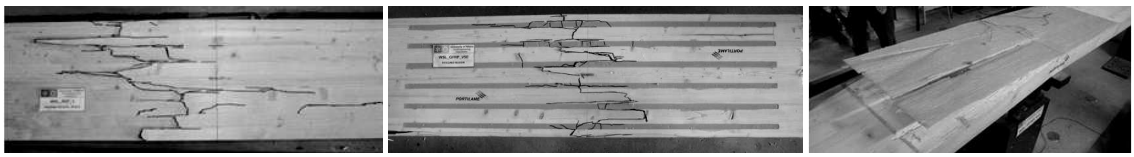

(a) (b) (c)

Figure 6. Typical failure modes: (a) REF, (b) NSM_40 and (c) EBR_20.

5 CONCLUSIONS

This work explores the potentialities of using FRP's systems for the flexural strengthening of continuous glulam slab strips, in terms of increasing the load carrying capacity, deformability and the bending moment redistribution capacity.

The NSM and EBR strengthening systems were designed to provide an increase of 20% and 40% of load carrying capacity of the reference slab. The aimed increase of the ultimate load was attained in the slabs strengthened according to the EBR technique, and did not occur in the NSM strengthened slabs.

However, the NSM strengthening technique has increased significantly the deformational capacity of these statically indeterminate structural systems, leading to a moment redistribution

that attained 25% in the slab strengthened with the highest percentage of FRP. In both slabs strengthened according to the EBR technique the moment redistribution was 9%.

Due to the intensive cracking process before the rupture of the FRP systems in the NSM flexurally strengthened slabs, a pronounced nonlinear branch between the applied load and the deflection occurred before the ultimate deflection. Therefore this technique has provided a significant increase in terms of deflection capacity. In fact, the two span unstrengthened glulam slab strips (reference slabs) presented an almost linear relationship between the applied load and the deflection up to failure, with a quite brittle failure mode, which deformational response was similar to the one registered in the slabs strengthened according to the EBR technique.

ACKNOWLEDGEMENTS

The present work is part of a research project was supported by the programs COMPETE and FEDER, project number PTDC/ECM/74337/2006, from the Portuguese Science and Technology Foundation (FCT). The authors also like to thank all the companies that have been involved supporting and contributing for the development of this study, mainly: INEGI, S&P® Reinforcement, Portilame, MAPEI and Rothoblaas.

REFERENCES

ACI 440.2R-08 (2008) "Guide for the Design and Construction of Externally Bonded FRP Systems for Strengthening Concrete Structures", *Reported by ACI Committee 440*, American Concrete Institute, 80 pp.

Brody, J., Richard, A., Sebesta, K., Wallace, K., Hong, Y., Lopez-Anido, R., Davids, W., and Landis, E. (2000) "FRP-wood-concrete composite bridge girders", *Structures of Structures Congress 2000 - Advanced Technology in Structural Engineering*, ASCE, Reston, Va.

Dagher, H.J., and Lindyberg, R. (1999) "FRP reinforced wood in bridge applications", *1st RILEM Symposium on Timber Engineering*, Cachan Cedex, France, 591–598.

Dagher, H.J., Kimball, T., Abdel-Magid, B., and Shaler, S.M. (1996) "Effect of FRP reinforcement on low-grade eastern hemlock glulams" *National Conf. on Wood Transportation Structures*, 9 pp.

Dagher, H.J., Poulin, J., Abdel-Magid, B., Shaler, S. M., Tjoelker, W., and Yeh, B. (1998) "FRP reinforcement of Douglas fir and western hemlock glulam beams", *International Composites Expo '98*, 22C, 1–4.

Davalos, J.F., Barbero, E., and Munipalle, U. (1992) "Glued-laminated timber beams reinforced with E-glass/polyester pultruded composites" *Structures Congress X*, 47–50.

EN 408:2003, "Timber structures - Structural timber and glued laminated timber. Determination of some physical and mechanical properties", European Committee for Standardization (CEN).

ISO 527-2:1993, "Plastics - Determination of tensile properties - Part 2: Test conditions for moulding and extrusion plastics", International Organization for Standardization.

ISO TC 71/SC 6 N Part 1:2003, "Non-conventional reinforcement of concrete-test methods: Fiber reinforced polymer (FRP) bars", International Organization for Standardization.

ISO TC 71/SC 6 N Part 2:2003, "Non-conventional reinforcement of concrete-test methods: Fiber reinforced polymer (FRP) sheets. International Organization for Standardization.

Jorge, M.A.P. (2011) "Experimental behavior of glulam-FRP systems", MSc Dissertation, Department of Civil Enginerring, University of Minho, 247 pp.

Lopez-Anido, R., and Xu, H. (2002) "Structural characterization of hybrid fiber-reinforced polymer-glulam panels for bridge decks", *Jounal of Composites for Construction*, 6(3): 194–203.

NP EN 1194:1999, "Estruturas de madeira. Madeira lamelada-colada. Classes de resistência e determinação de valores característicos. Timber structures. Glulam wood. Strength classes and determination of the chacateristic values", Instituto Português da Qualidade, Lisbon. (in Portuguese)

NP EN 1194:1999, Estruturas de madeira. Madeira lamelada-colada. Classes de resistência e determinação de valores característicos. IPQ, Lisbon. (*In Portuguese*)

Tingley, D.A., Gai, C., and Giltner, E. (1997) "Testing methods to determine properties of fiber reinforced plastic panels used for reinforcing glulams", *Jounal of Composites for Construction*, 1(4): 160–167.